

Research Article: Confirmation | Integrative Systems

Developmental nicotine exposure alters synaptic input to hypoglossal motoneurons, and is associated with altered function of upper airway muscles

https://doi.org/10.1523/ENEURO.0299-19.2019

Cite as: eNeuro 2019; 10.1523/ENEURO.0299-19.2019

Received: 31 July 2019 Revised: 3 October 2019 Accepted: 13 October 2019

This Early Release article has been peer-reviewed and accepted, but has not been through the composition and copyediting processes. The final version may differ slightly in style or formatting and will contain links to any extended data.

Alerts: Sign up at www.eneuro.org/alerts to receive customized email alerts when the fully formatted version of this article is published.

Copyright © 2019 Wollman et al.

This is an open-access article distributed under the terms of the Creative Commons Attribution 4.0 International license, which permits unrestricted use, distribution and reproduction in any medium provided that the original work is properly attributed.

1	1. Manuscript Title (50 word maximum)
2	Developmental nicotine exposure alters synaptic input to hypoglossal motoneurons, and is
3	associated with altered function of upper airway muscles
4	
5	2. Abbreviated Title (50 character maximum)
6	Perinatal nicotine and upper airway motor control
7	r erniatar meotine and apper an way motor control
8	3. List all Author Names and Affiliations in order as they would appear in the published
9	article
10	Lila Wollman ¹
11	Iordan Clarke ¹
	Claire DeLucia ¹
12	
13	Richard B. Levine ^{1,2}
14	Ralph F. Fregosi ^{1,2}
15	¹ Department of Physiology; ² Department of Neuroscience. The University of Arizona,
16	Tucson, Arizona, USA
17	
18	4. Author Contributions: LW, RBL & RFF wrote the paper & designed the research; LW, JC
19	& CD Performed Research; LW, JC, CD & RFF analyzed the data
20	
21	5. Correspondence should be addressed to (include email address)
22	Ralph F. Fregosi, PhD, Department of Physiology, University of Arizona, College of
23	Medicine,1501 N. Campbell Ave, Tucson, AZ 85724, USA
24	Email: <u>fregosi@email.arizona.edu</u>
25	
26	6. Number of Figures 10
27	7. Number of Tables 5
28	8. Number of Multimedia 0
29	9. Number of words for Abstract 244
30	10. Number of words for Significance Statement 118
31	11. Number of words for Introduction 508
32	12. Number of words for Discussion 2358
33	13. Acknowledgements
34	We wish to thank Seres Cross for her expert technical assistance.
35	14. Conflict of Interest: A. Authors report no conflict of interest
36	15. Funding sources: Eunice Kennedy Shriver National Institute of Child Health and
37	Human Development; NICHD 5R01HD071302-07.
38	
39	
40	

41 Abstract

42 Nicotine exposure during the fetal and neonatal periods (Developmental nicotine 43 exposure, DNE) is associated with ineffective upper airway protective reflexes in infants. This could be explained by desensitized chemoreceptors and/or mechanoreceptors. 44 45 diminished neuromuscular transmission or altered synaptic transmission among central 46 neurons, as each of these systems depend in part on cholinergic signaling through 47 nicotinic acetylcholine receptors (nAChRs). Here we showed that DNE blunts the 48 response of the genioglossus muscle to nasal airway occlusion in lightly anesthetized 49 rat pups. The genioglossus muscle helps keep the upper airway open and is innervated 50 by hypoglossal motoneurons (XIIMNs). Experiments using the phrenic nerve-51 diaphragm preparation showed that DNE does not alter transmission across the 52 neuromuscular junction. Accordingly, we used whole cell recordings from XIIMNs in 53 brainstem slices to examine the influence of DNE on glutamatergic synaptic 54 transmission under baseline conditions and in response to an acute nicotine challenge. 55 DNE did not alter excitatory transmission under baseline conditions. Analysis of 56 cumulative probability distributions revealed that acute nicotine challenge of P1-P2 57 preparations resulted in an increase in the frequency of nicotine-induced glutamatergic 58 inputs to XIIMNs in both control and DNE. By contrast, P3-P5 DNE pups showed a 59 decrease, rather than an increase in frequency. We suggest that this, together with 60 previous studies showing that DNE is associated with a compensatory increase in 61 inhibitory synaptic input to XIIMNs, leads to an excitatory-inhibitory imbalance. This 62 imbalance may contribute to the blunting of airway protective reflexes observed in 63 nicotine exposed animals and human infants.

65 Significance statement

66 The number one risk factor for sudden infant death (SIDS) is maternal smoking. While 67 the use of nicotine delivery devices such as e-cigarettes is increasing among women of 68 childbearing age, reflecting the belief that the use of nicotine alone is safer than 69 tobacco, SIDS deaths are not decreasing, suggesting that nicotine is the link between 70 maternal smoking and SIDS. Here we show that perinatal nicotine exposure alters a 71 major motor pathway responsible for upper airway patency during sleep. We also 72 introduce an animal model that is well suited to probing the mechanisms underlying the 73 link between maternal nicotine consumption and SIDS, and a phenotype that nicely 74 models key aspects of the events believed to give rise to SIDS.

75

76 Introduction

77 Hypoglossal motoneurons (XIIMNs) innervate the muscles of the tongue, which 78 are critically important in the maintenance of airway patency during breathing (Lowe, 79 1980). The breathing-related drive to the tongue muscles relies on the appropriate 80 timing and strength of XIIMN output, which is strongly influenced by the balance of 81 excitatory and inhibitory fast-synaptic inputs that the motoneurons receive (Berger, 82 2011), and a functionally viable neuromuscular junction. Environmental factors, such as 83 exposure to nicotine in the perinatal period, can alter the course of normal nervous 84 system development. This is attributed to nicotine's action on nicotinic acetylcholine 85 receptors (nAChRs), which are well known for their role in modulating synaptic 86 transmission in the brain (Wonnacott et al., 2005) and neuromuscular junction (Wood

87	and Slater, 2001). In terms of tongue muscle function in nicotine-exposed human	
88	neonates, there are limited though interesting observations. These include an increased	
89	incidence of obstructive apneas (Kahn et al., 1994) and hypoplasia and immaturity of	
90	XIIMNs (Ottaviani et al., 2006; Lavezzi et al., 2010). In contrast with these limited data	
91	from human neonates, there is a considerable body of work on the influence of	
92	developmental nicotine exposure (prenatal exposure with continued exposure in the first	
93	week of life, DNE) on the structure and function of XIIMNs. For example, XIIMNs from	
94	DNE animals have a significantly more complex dendritic arbor than cells from control	
95	animals on postnatal days 1-2 (P1-P2), but by P3-4 the arbor is less complex	
96	suggesting altered neuronal development over the first week of life (Powell et al., 2016).	
97	As for intrinsic properties, XIIMNs from DNE animals are hyperexcitable (Pilarski et al.,	
98	2011) and show increased GABAergic inhibition (Jaiswal et al., 2016; Wollman et al.,	
99	2018a). We believe that the increase in GABAergic inhibition to nicotine-exposed	
100	XIIMNs is consistent with a homeostatic mechanism aimed at mitigating the increased	
101	intrinsic excitability. However, a homeostatic response to the increased cell excitability	
102	may also include reductions in excitatory synaptic input to XIIMNs.	
103	The experimental results reported here were designed to gain a further	
104	understanding of how DNE impacts tongue muscle function at rest and in response to a	
105	respiratory challenge, the nature of excitatory synaptic inputs to XIIMNs, and the	
106	integrity of the neuromuscular junction. First, tongue muscle function was evaluated in	
107	vivo by recording the breathing-related tongue muscle EMG before, during and after a	
108	period of airway occlusion in lightly anesthetized neonatal rats. Next, since hypoxia and	

109 hypercapnia (as occurs during airway occlusion) is associated with increased

110 acetylcholine release (Metz, 1966; Huckstepp et al., 2016), and DNE is known to alter 111 nAChR function throughout the brain (Wonnacott, 1990; Wonnacott et al., 1990; Gentry 112 and Lukas, 2002), we hypothesized that DNE may change how nAChR activation 113 modulates excitatory fast-synaptic inputs to XIIMNs. Accordingly, we evaluated the 114 amplitude and frequency of AMPA receptor-mediated glutamatergic synaptic inputs to 115 XIIMNs at baseline and in response to acute activation of nAChRs. Finally, using the 116 hemi diaphragm-phrenic nerve preparation as a model, we probed the effects of DNE 117 on the integrity of the neuromuscular junction by measuring neuromuscular 118 transmission failure and susceptibility to fatigue.

119

120 Materials and Methods

121 Animals. We used a total of 195 Sprague-Dawley rat pups of either sex, ranging 122 in age from postnatal day one (P1) through P7, which in terms of comparable brain 123 development in humans corresponds roughly to the 23rd week of gestation through birth 124 (Semple et al., 2013). An equal number of control and nicotine exposed animals were 125 used. All neonates were born via spontaneous vaginal delivery from pregnant adult 126 female rats purchased from Charles River Laboratories (Wilmington, MA). Neonates 127 were housed with their mothers and siblings in the animal care facility at the University 128 of Arizona under a 12:12 hour light/dark cycle (lights on 07:00 h), in a quiet room 129 maintained at 22 °C and 20-30% relative humidity, and with water and food available ad 130 libitum. All procedures and protocols described were approved by the University of 131 Arizona Institutional Animal Care and Use Committee, and in accordance with National 132 Institutes of Health guidelines.

133	Developmental nicotine exposure. Pregnant Sprague-Dawley dams (Charles
134	River Laboratories) were anesthetized with a subcutaneous injection of ketamine (25
135	mg/kg), xylazine (8.0 mg/kg) and acepromazine (1 mg/kg) and an Alzet 1007D mini-
136	osmotic pump (Alzet Corp., CA, USA) was implanted subcutaneously on gestational day
137	5. A subcutaneous injection of buprenorphine (0.5 mg/kg) was given to control
138	postoperative pain. The 28-day pump exposes the pup via the placenta throughout the
139	remainder of gestation (approximately 16 days), and via breast milk after birth, and
140	these successive pre and postnatal exposures define DNE. The pump was loaded to
141	deliver an average dose of 6 mg/kg/day of nicotine bitartrate. This dose produces
142	plasma cotinine (a metabolic by-product of nicotine) levels in the pups ranging from 60-
143	92 ng/ml (Powell et al., 2016), which is comparable to that seen in the plasma of human
144	infants born to mothers who are considered moderate smokers (Berlin et al., 2010).
145	Control animals were obtained from pregnant dams implanted with an Alzet pump filled
146	with saline (sham control). Consistent with our previous studies, there were no
147	systematic differences in measured variables between sham control and animals
148	obtained from pregnant dams that did not undergo pump implantation (true
149	control). Pregnant dams were euthanized on postnatal day 7 using institutionally and
150	federally-approved procedures.
151	In vivo studies. These studies were designed to test the hypothesis that DNE is
152	associated with decreased drive to the tongue muscles in response to airway occlusion
153	(i.e., the model of an external stressor). Neonatal rat pups ranging in age from P3-P7
154	were lightly anesthetized with a mixture of ketamine (30 mg/mL), xylazine (6 mg/mL)

155 and acepromazine (3 mg/mL), injected subcutaneously at a volume corresponding to

156 approximately 0.35 µL/g body weight. Pain sensitivity was checked via multiple paw 157 pinches initiated 10 minutes after the time of injection. Supplemental anesthetic was 158 added until paw retraction upon pinching was abolished. Whole muscle 159 electromyographic (EMG) activity of the genioglossus muscle (GG, a tongue protrudor 160 muscle) was recorded using fine wire electrodes inserted into the area underneath the 161 tip of the mandible (Fig. 1A) (Bailey et al., 2005; Rice et al., 2011). An additional hook 162 wire electrode placed into the scruff of the neck near the animal's ear served as an 163 electrical ground. EMG signals were filtered (30-3000 Hz), amplified (Grass P122 AC 164 amplifiers) and sent to an A/D converter (Cambridge Electronic Design (CED); model 165 1401), which sampled the signal at a rate of 8333 Hz. After the experiment, animals 166 were killed with an overdose of pentobarbital sodium, and electrode location was 167 confirmed by dissection. Data were accepted only if we could confirm that the wires 168 were in the GG muscle. In four animals we also inserted pairs of fine wire electrodes 169 into the diaphragm just beneath the lower ribs, to document that overall respiratory 170 motor drive persisted during airway occlusion (Fig. 1B).

171 After implantation of the EMG electrodes, the animal was inserted into a 32 ml 172 head-out plethysmograph in the supine position (Fig. 1A). A neck seal was formed with 173 latex, allowing the animal to breathe normally from the room air, with the thorax and 174 abdomen isolated in the sealed chamber. When the animal inhales, its thorax expands, 175 forcing gas out of the sealed chamber. The gas flow entering and leaving the chamber 176 was measured with a pneumotach (Hans-Rudolph) connected to a pressure transducer 177 (Validyne, sensitivity +/- 2 cmH2O), and from this we obtained a recording that is 178 proportional to respiratory airflow (bottom trace in Fig. 1B). This signal was passed to

179 an analog integrator (Grass) that computed the area under the inspired segment of the 180 curve, providing a measure of the inspired tidal volume (Fig. 1B, third trace from the 181 top). We calibrated tidal volume by injecting known volumes of gas into the chamber 182 with a 50 µL Hamilton syringe. The pressure, tidal volume and EMG signals were sent 183 to an analog-to-digital converter (Cambridge Electronics Design), displayed in real time 184 on a computer monitor (Spike II software) and stored on a hard drive for subsequent 185 offline analysis. The plethysmograph temperature was maintained between 32 and 186 34°C using a temperature probe and heat lamp. This range is within the thermoneutral 187 zone for neonatal rats (Mortola, 1984; Mortola and Tenney, 1986; Sant'Anna and 188 Mortola, 2003; Mortola, 2004). Though we did not measure body temperature, previous 189 studies show that baseline body temperature is the same in control and DNE rat pups 190 (Ferng and Fregosi, 2015).

191 After baseline recordings were completed, the animal was challenged with 15 192 sec of nasal occlusion (Fig. 1B), resulting in strong breathing efforts but an absence of 193 lung inflation, as well as hypoxia, hypercapnia and acidosis. Measurement of peak EMG 194 activity, tidal volume and breathing frequency throughout the period of nasal occlusion 195 were organized into bins corresponding to five, 20% segments of occlusion time. The 196 EMG activity was normalized in each animal by first detecting the largest burst recorded 197 during the experimental procedure and assigning a value of 1.0 to that burst, which 198 represents the peak activity in each experiment. The average burst amplitude within 199 each 20%-time bin was expressed as a fraction of the maximal burst amplitude (e.g., 200 Fig. 1C). We also measured the time between the onset of nasal occlusion and the 201 onset of the first EMG burst during occlusion, and defined this as the response latency

(e.g., Fig. 2). Changes in EMG activity during nasal occlusion were analyzed with twoway ANOVA, with time and treatment the main factors. Post hoc analysis was by
Tukey's test. The difference in EMG onset latency was tested with the unpaired t-test.
P < 0.05 was taken as the threshold for statistical significance (Table 4).

In the course of working out the *in vivo* techniques, we completed 15-sec nasal occlusion trials in 135 animals. Only a minority of these animals qualified for the main analysis, which required both high quality plethysmographic and EMG recordings (9 control, 11 DNE); the remainder were not used in the main analysis. However, we did find that 12 of the 135 animals failed to recover from nasal occlusion, and as shown in Fig. 3., the majority of these were DNE animals.

212 In vitro study A-whole cell voltage clamp recordings of XIIMNs in medullary slice 213 preparations. These experiments were designed to examine the influence of DNE on 214 AMPA-mediated glutamatergic synaptic input to XIIMNs. As indicated below, we studied 215 both spontaneous excitatory post synaptic currents (sEPSCs) and miniature EPSCs 216 (mEPSCs) inputs This dual focus is important, as sEPSCs reflect both action potential-217 mediated glutamate release, as well as inputs due to the random, guantal release of 218 glutamate from presynaptic terminals. Moreover, nAChRs are located presynaptically 219 on the soma, dendrites and axon end-terminals of glutamatergic neurons as well as 220 postsynaptically on XIIMNs, and exposure to nicotine could alter nAChRs in all of these 221 locations. Therefore, recording both miniature and spontaneous events can help 222 determine whether the actions of DNE on XIIMNs are presynaptic or postsynaptic. 223 Pups of either sex were removed from their cages, weighed, anesthetized on ice

224 and decerebrated at the coronal suture. The vertebral column and ribcage were

225	exposed and placed in cold (4-8 $^\circ\text{C})$ oxygenated (95% O_{2^-} 5% $CO_2)$ artificial
226	cerebrospinal fluid (aCSF), composed of the following (in mM): 120 NaCl, 26 NaHCO ₃ ,
227	30 glucose, 1 MgSO ₄ , 3 KCl, 1.25 NaH ₂ PO ₄ , and 1.2 CaCl ₂ with pH adjusted to 7.4
228	and osmolarity to 300-325 mOsm. The brainstem was extracted and glued to an agar
229	block, rostral surface up, and 2-3 transverse medullary slices (300-500mM) containing
230	the hypoglossal motor nucleus were cut in a vibratome (VT1000P, Leica) filled with ice-
231	cold aCSF. The slices were then transferred to an equilibration chamber containing
232	fresh, oxygenated, room temperature aCSF and allowed to recover for 1.5 hours before
233	recording.
234	Equilibrated slices were transferred to a recording chamber maintained at 27 $^\circ\text{C}$
235	(TC-324B temperature controller, Warner Instrument Corporation) and perfused

2 236 with oxygenated (95% O₂/5% CO₂) aCSF at a rate of 1.5-2 ml/min. XIIMNs were 237 visualized with an Olympus BX-50WI fixed-stage microscope (40x water-immersion 238 objective, 0.75 N.A.) with differential contrast optics and a video camera (C2741-62, 239 Hamamatsu). Recordings were made with glass pipettes (tip resistance 3-7 M Ω) pulled 240 from thick-walled borosilicate glass capillary tubes (OD: 1.5 mm, ID: 0.75 mm). We used 241 a CsCl based intracellular solution containing (in mM): 130 CsCl, 5 NaCl, 2 MgCl₂, 242 1 CaCl, 10 HEPES, 2 ATP-Mg, 2 Sucrose, with pH adjusted to 7.2 and osmolarity of 243 250-275 mOsm. Under these conditions, the chloride reversal potential is approximately 244 0 mV (actual value = -2.8 mV) and therefore both excitatory and inhibitory post-synaptic 245 currents are inward at a holding potential of -75 mV. Filled pipettes were attached to a head stage mounted in a micromanipulator (MP-225, Sutter Instrument Company). The 246

248digitized with a Digidata 1440A A/D converter (Molecular Devices).249The following procedures pertain to all recordings. First XIIMNs were identified250based on their size, shape and location. We targeted the cell soma with the pipette and251after a gigaohm seal was achieved the membrane was ruptured by suction. After a 5-252minute equilibration period to confirm a stable recording, we pharmacologically253isolated AMPA receptor-mediated sEPSCs using D-(-)-2-Amino-5-phosphonopentanoic254acid (AP-5), strychnine hydrochloride, and bicuculline methiodide to antagonize the255NMDA receptors the glycine receptors, and the GABAA receptors, respectively (Table2561). In the first set of experiments, sEPSCs were recorded for three minutes at baseline

247

isolated AMPA receptor-mediated sEPSCs using D-(-)-2-Amino-5-phosphonopentanoic acid (AP-5), strychnine hydrochloride, and bicuculline methiodide to antagonize the NMDA receptors the glycine receptors, and the GABA_A receptors, respectively (Table 1). In the first set of experiments, sEPSCs were recorded for three minutes at baseline, 257 and then for an additional three minutes during bath application of nicotine (acute 258 nicotine challenge). This protocol was followed by five minutes of washout with aCSF. 259 In the second set of experiments we examined the influence of DNE on mEPSCs 260 both before and after an acute nicotine challenge. After a stable recording was 261 achieved, we blocked NMDA, GABAA and glycine receptors, as above, to isolate 262 AMPA-mediated excitatory events. This cocktail was superfused for three minutes, 263 followed by the addition of tetrodotoxin (TTX) for two minutes to block action potential 264 firing (Table 1). AMPA receptor-mediated mEPSCs were recorded at baseline for three 265 minutes, after which nicotine bitartrate was added to the superfusate. mEPSCs were 266 recorded for an additional three minutes in the presence of nicotine, followed by a five-267 minute washout period.

head stage was connected to a Multiclamp 700B amplifier, and the signals were

In a third set of experiments, to evaluate the influence of DNE on post-synaptic
 AMPA receptors, recordings were again made in the presence of AP-5, strychnine

270	hydrochloride, bicuculline methiodide, and TTX (Table 1). We then bath applied AMPA,
271	to activate post-synaptic AMPA receptors. Under these conditions, activation of the
272	AMPA receptors produces an inward current and the peak of this current was
273	measured. Post-synaptic currents were recorded in voltage clamp with
274	Clampex software (Molecular Devices, Sunnyvale, CA), and analyzed
275	with MiniAnalysis software (Synaptosoft, Decatur, GA, USA).
276	Drugs: Drugs were purchased from Sigma (St. Louis, MO, USA), except for
277	nicotine bitartrate (MP Biomedicals, LLC, Solon, OH, USA) and TTX (R&D Chemicals,
278	Minneapolis, MN, USA). All drugs were mixed in aCSF on the day of the experiment
279	from previously mixed aliquots that were frozen and stored at 0-2 $^\circ$ C. Antagonists were
280	used at concentrations known to be effective based on our previous studies or the
281	literature. Nicotine was used at the highest dose that produced presynaptic effects
282	(increased frequency of sEPSCs in pilot experiments) without producing a significant
283	inward current, which we found to be 0.5 $\mu M.$ This is important, as pilot studies showed
284	that higher concentrations of nicotine (1 mM, 10 mM, and 100 mM) activates
285	postsynaptic nAChRs and evokes an inward current, that decreases the ability to
286	discriminate sEPSCs /mEPSCs. AMPA was used at a concentration that produced an
287	approximately half maximal response (2.5 μM), based on dose response experiments
288	previously performed in our lab. The drug solutions were oxygenated and maintained at
289	27 °C and perfused into the recording chamber at a rate of 1.5-2 ml/min.
290	Data from a total of 72 cells are reported, with 36 cells from DNE neonates and
291	36 cells from control neonates. Cell numbers for each experiment are summarized in
292	Table 2. The average number of sEPSCs and mEPSCs evaluated per neuron is shown

293 in Table 4. At the end of each experiment, the resting membrane potential and input 294 resistance were measured again to confirm the health of the cell and that 295 the gigaohm seal was still intact. Because of the morphological differences seen in 296 neurons from DNE animals aged P1-2 compared to age P3-5 (Powell et al., 2016), we 297 analyzed our data within these two age groups. For all EPSCs, the inter-event interval 298 (IEI) and peak amplitude were measured during the minute before the nicotine 299 challenge, and throughout the second and third minutes of the challenge. For mEPSCs, 300 rise time was measured at these same time points. There were no differences for any of 301 these variables between the second and third minutes of nicotine challenge, so data 302 recorded in the third minute was used for analysis. Lastly, we measured the peak of the 303 whole cell inward current evoked by stimulation of postsynaptic AMPA receptors with 304 bath applied AMPA (e.g., Fig. 9A). 305 In vitro study B- hemi diaphragm-phrenic nerve preparation. To estimate the

306 influence of DNE on the integrity of the neuromuscular junction, and as a substitute for 307 the hypoglossal nerve-tongue neuromuscular junction (see Discussion), we used 308 neonatal rat (P1-P5) phrenic nerve-hemidiaphragm preparations. Diaphragm muscle 309 was excised and secured in a dish perfused with warmed (37 °C), oxygenated Krebs 310 solution, containing (in mM): 123 NaCl, 26 NaHCO₃, 30 glucose, 1 MgSO₄, 3 KCl, 1.25 311 NaH₂PO₄ and 1.2 CaCl], gassed with 95% O₂/5% CO₂, with pH adjusted to 7.45-7.5. 312 Force was measured with a transducer (Kent Scientific) attached to the central tendon 313 of the hemi diaphragm, and the phrenic nerve was drawn into a suction electrode, which 314 was referenced to a bath ground and connected to a stimulator (Grass S88). Two 315 silver/silver-chloride discs were pinned to the bath on either side of the muscle strip and

connected to a second channel on the stimulator for direct depolarization of the muscle
fibers, bypassing the neuromuscular junction. Force and the output of the stimulator
were digitized and monitored on a computer using Spike II hardware and software
(Cambridge Electronics Design, London, UK).

320 To measure muscle twitch force and contraction speed in response to direct 321 muscle stimulation we delivered single, 0.2 ms supramaximal pulses to the bath 322 electrodes. We also measured the decline in force following 5 min of intermittent, 323 supramaximal direct muscle stimulation, while in another set of animals we stimulated 324 the phrenic nerve. Both muscle and nerve were stimulated with 0.2 ms pulses, delivered 325 in 330 ms trains at 40 Hz, with a train delivered every 2 sec. In additional sets of 326 animals, we estimated the contribution of neuromuscular transmission to force loss by 327 applying stimulus trains to the phrenic nerve, as above, while superimposing direct 328 muscle stimulation every 15 sec. Neuromuscular transmission failure was computed by 329 comparing the force loss during nerve stimulation with that evoked by direct muscle 330 stimulation (see Fig. 10C), as described by others (Aldrich et al., 1986; Fournier et al., 331 1991). Force decline due to neuromuscular transmission failure = (force loss during 332 nerve stimulation - force loss during muscle stimulation) / (1- force loss during muscle 333 stimulation).

<u>Statistics</u>. A brief summary of the statistical analysis used in each of the three experimental series is given in Table 2. <u>In vivo experiments</u>. Changes in EMG activity during nasal occlusion were analyzed with two-way ANOVA, with time and treatment the main factors. Post hoc analysis was by Tukey's test. The difference in EMG onset latency was tested with the unpaired t-test. P < 0.05 was taken as the threshold for

statistical significance (Table 2). Differences in the number of failed autoresuscitations
was compared between groups using a Chi square analysis (Table 2).

In vitro study A-whole cell voltage clamp recordings of XIIMNs in medullary slice 341 342 preparations. Differences in baseline variables including age, weight, resting membrane 343 potential, and input resistance were evaluated between treatment groups, and between 344 age groups within a treatment group, by comparing the means from each group with a 345 two-way ANOVA, followed by Tukey's post hoc test for multiple comparisons (Table 2). 346 We analyzed the IEI and amplitude for both sEPSCs and mEPSCs in two ways 347 (see Table 2). First, the IEI and amplitude of all sEPSCs/mEPSCs from all cells within 348 an age or treatment group were used to construct a cumulative probability distribution 349 using Prism (GraphPad Software, Inc., La Jolla, CA) (e.g., Figures 5 and 7). We 350 expressed the cumulative probability as fractions ranging from 0 to 1, such that a value 351 of 0.5 defines the midpoint of the normalized EPSC amplitude or frequency distribution. 352 In these graphs, the y-axis value is the fraction of events that lies at or below the 353 corresponding x-axis value. To compare the IEI and amplitude distributions between 354 baseline conditions and during acute nicotine application, we performed a two-sample 355 Kolmogorov-Smirnov (K-S) test using SPSS (IBM, Armonk, NY). 356 Second, in each cell we recorded the median value of IEI and the event 357 amplitude for every event, both at baseline and during acute nicotine challenge in both 358 age and treatment groups. We then ran a separate mixed model, three-way factorial 359 ANOVA for each of these variables, with the main factors the treatment group (control 360 vs. DNE), age (P1-P2 vs. P3-P5) and experimental condition (baseline vs. acute

361 nicotine challenge). When the ANOVA was significant, we conducted post hoc

analyses using the Holm-Sidak multiple comparisons test, with the alpha level set at P <
0.05. We used an unpaired t-test to compare the mean peak current in control and
nicotine exposed cells (Table 2). We note that this approach is considerably more
conservative than the analysis of cumulative probability distributions, which is the most
popular technique for analyzing excitatory and inhibitory synaptic potentials (Henze et
al., 1997). This is because probability distributions typically pool all events from all cells
into a single distribution, which inflates the statistical power.

<u>In vitro study B- hemi diaphragm-phrenic nerve preparation.</u> Average values for
 force loss in response to nerve stimulation, muscle stimulation and estimates of
 neuromuscular transmission failure in control and DNE animals were compared with the
 unpaired t-test. As above, P < 0.05 was the threshold for statistical significance (Table
 Average data is reported as the mean ± SD throughout the manuscript.

374

376

375 Results

In vivo studies: Influence of DNE on tongue muscle EMG activity in

377 response to airway obstruction. We began our study by assessing the impact of 378 DNE on neural drive to the GG muscle of the tongue, which is innervated by XIIMNs 379 and plays a major role in keeping the upper airway open (Remmers et al., 1978). We 380 did this by challenging the system with a 15 sec nasal occlusion, initiated during the 381 expiratory period. Airway occlusion in neonates typically results in a strong increase in 382 drive to the muscles of breathing. The representative recordings in Fig. 1B show that 383 nasal occlusion is associated with a monotonic increase in the EMG activity of both the 384 diaphragm and the GG. The group average data (Fig. 1C) show that the increase in

GG EMG activity during occlusion was significantly blunted in the DNE animals,
consistent with a reduced excitation of XIIMNs. In addition to the reduced amplitude of
the GG EMG during occlusion, the onset latency was longer in DNE animals (P <
0.001), as shown in the representative recordings in Figs. 2A and 2B, with individual
and mean values shown in Fig. 2C. This observation is consistent with a DNEmediated blunting of excitatory drive to hypoglossal motoneurons during airway
occlusion.

392 As indicated in methods, we did the nasal occlusion test in 135 neonates and 393 noted that 12 of the 135 never recovered, and instead entered a state characterized by 394 terminal gasping. The pattern of breathing in animals that did not recover most often 395 approximated that shown in Fig. 3A, in that long periods of apnea were terminated 396 following bursts of GG activity. Fig. 3A also shows that, at times, multiple bursts of GG 397 EMG activity were required to terminate an apnea. These observations are consistent 398 with upper airway obstruction, as the bursting pattern of GG EMG activity suggests that 399 the XIIMNs were receiving drive from the respiratory central pattern generator but 400 airflow was not detected. Interestingly, of the 12 neonates that entered this state of 401 unstable breathing, nine were DNE animals (Fig. 3B). This difference in the ability to 402 survive nasal airway occlusion was statistically significant by Chi square analysis (Chi 403 statistic = 3.594, Z score = 1.896, P = 0.0290), with an adjusted odds ratio of 3.5.

404 In vitro study A-whole cell voltage clamp recordings of XIIMNs in medullary
405 slice preparation.

406 <u>Influence of DNE on age, weight, Vm and input resistance</u>. The age and weight
 407 of the animals used in these experiments are shown in Table 3. The age of the animals

408 studied in each treatment group was the same, eliminating age bias in the results. The 409 older animals were heavier, as expected, but there were no differences in body weight 410 between control and DNE animals in either age group. There were also no effects of 411 age or treatment for either Vm or input resistance (Table 3). We note that the values for 412 input resistance are higher than values recorded with standard intracellular solutions, 413 but are consistent with values recorded with Cs-based intracellular solutions, as used 414 here.

Influence of DNE on the frequency and amplitude of glutamatergic sEPSCs in

416 brain stem slices. To evaluate the influence of DNE on network level AMPA receptor-417 mediated synaptic events under baseline conditions, we evaluated differences in the 418 inter-event intervals (IEIs) and the amplitude of sEPSCs in control and DNE cells. The 419 upper traces in Fig. 4A and 4B are example recordings of glutamatergic sEPSCs from 420 one control and one DNE cell under baseline conditions; both recordings were obtained 421 from a P4 animal. There are no obvious differences in the traces from control and DNE 422 cells at baseline, which is consistent with comparisons of the mean data showing no 423 significant differences for baseline sEPSC IEI (Fig. 8A) or amplitude (Table 3) between 424 control and DNE cells, in either of the age groups.

We then studied the influence of an acute nicotine challenge on the frequency
and amplitude of sEPSCs. The tracings in Fig. 4 (recordings labeled 0.5μM Nicotine)
show a modest increase in sEPSC frequency with nicotine challenge in the control cell,
while the DNE cell showed little change in amplitude, but a decrease in frequency.
Examination of cumulative probability curves in animals aged P1-P2 (Figs. 5A and 5B)

430 show that the distributions shifted to the left, to lower IEIs (higher frequency) with acute

431	nicotine challenge in both control (P=0.049, based on 675 and 749 events at baseline
432	and with acute nicotine challenge, respectively) and DNE cells (P<0.0001, 871 events at
433	baseline, 1170 events with nicotine challenge). In animals aged P3-P5, nicotine
434	challenge again shifted the cumulative probability distributions to the left in control
435	animals (Fig. 5C; P<0.0001, based on 570 and 1271 events analyzed at baseline and
436	during nicotine challenge, respectively). However, in the P3-P5 DNE animals acute
437	nicotine challenge shifted the curve to the right, indicating a slowing, rather than an
438	increase in sEPSC frequency (Fig. 5D; P=0.012, based on 678 and 501 events
439	analyzed at baseline and during nicotine challenge, respectively).
440	We also analyzed the group mean data for all events by first averaging all events
441	in each cell, followed by calculation of the grand mean value within each of the four age
442	and treatment groups (Fig. 8A). The group mean data show that in control cells, acute
443	nicotine challenge had no significant effect on the IEI at either age (Fig. 8A). In
444	contrast, whereas acute nicotine challenge had no significant effect on DNE cells at
445	ages P1-2, it was associated with an increase in sEPSC IEI in cells from animals aged
446	P3-P5, indicating a significant decrease in the frequency of sEPSCs (P = 0.0021, Fig.
447	8A). In addition, the change in IEI in the DNE cells from P1-2 and P3-5 animals is
448	significantly different (P = 0.0001, Fig. 8A). The IEI in DNE cells from P3-5 pups was
449	also different from the IEI in cells from P3-5 control cells (P = 0.0006, Fig. 8A). As with
450	control cells, nicotine challenge had no effect on sEPSC amplitude in cells from DNE
451	animals at either age, and this was true whether we analyzed the entire population of
452	events with cumulative probability analyses (data not shown), or with ANOVA based on
453	the average data in each age and treatment group (Table 5).

454 Frequency, amplitude and rise time of glutamatergic mEPSCs. We also 455 evaluated how DNE affects the frequency, amplitude and rise time of AMPA receptor-456 mediated mEPSCs, which represent the random, guantal release of glutamate from 457 presynaptic terminals. The upper traces in Fig. 6A and 6B are mEPSCs recorded under 458 baseline conditions, while the lower traces were recorded during acute nicotine 459 challenges. Figures 6A and 6B are from a control and DNE animal, both studied on P2. 460 Examination of cumulative probability curves in animals aged P1-P2 (Figs. 7A 461 and 7B) show that the distributions shifted to the left, to lower IEIs (higher frequency) 462 with acute nicotine challenge in both control (P<0.0001, based on 168 and 221 events 463 at baseline and with acute nicotine challenge, respectively) and DNE cells (P<0.0001, 464 169 events at baseline, 361 events with nicotine challenge). In animals aged P3-P5, 465 nicotine challenge again shifted the cumulative probability distributions to the left in 466 control animals (Fig. 7C; P=0.004, based on 91 and 164 events analyzed at baseline 467 and during nicotine challenge, respectively). However, in the P3-P5 DNE animals acute 468 nicotine challenge did not affect the cumulative probability distribution of mEPSCs 469 significantly (Fig. 7D; P=0.066, based on 186 and 202 events analyzed at baseline and 470 during nicotine challenge, respectively). 471 Analysis of the group mean data did not reveal significant differences in either 472 the frequency (Fig. 8B) or amplitude (Table 5) of mEPSCs in either control or DNE cells, 473 both at baseline and with acute nicotine challenge. Similarly, there were no significant

474 differences for mEPSC rise time either between treatment groups at baseline, or

475 between baseline and nicotine challenge within a treatment group (Table 5).

476	Influence of DNE on postsynaptic AMPA receptors. To gain a more complete
477	understanding of DNE-mediated effects on AMPA receptor function, we obtained
478	recordings from XIIMNs and measured the peak inward current that was produced by
479	bath application of 2.5 μM AMPA in the presence of AP-5, strychnine hydrochloride,
480	bicuculline methiodide, and TTX (Table 1). Figure 6A shows an example trace of the
481	inward current that results from activation of the postsynaptic AMPA receptors with bath
482	application of 2.5 μM AMPA in a control cell from a P1 animal. The average peak
483	amplitude of the inward current was the same in DNE and control cells in both age
484	groups, and there were no differences in current amplitude with age in either control
485	cells or DNE cells (Fig. 9B).
486	In vitro study B- Influence of DNE on diaphragm muscle contractile

487 properties and the susceptibility to fatigue. Contractile properties (mean ± SD) 488 including peak twitch tension (Control, 2.5 ± 1.2 g; DNE 2.6 ± 1.3 g), time to peak 489 tension (Control, 50 \pm 10 ms; DNE 60 \pm 10 ms), and ½ relaxation time (Control, 70 \pm 20 490 ms; DNE 60 ± 20 ms) were the same in diaphragm strips from control and DNE 491 animals. We note that our values for each of these variables are similar to those 492 reported in 7 day-old neonatal rats (Zhan et al., 1998). Figure 7A is an example of the 493 force decline recorded in diaphragm muscle strips following repetitive trains of phrenic 494 nerve stimulation, while Fig. 10C is an example of the protocol used to estimate the 495 contribution of neuromuscular transmission failure to the decline in force. Note that 496 direct muscle stimulation was superimposed on phrenic nerve stimulation approximately 497 every 15 sec, and the difference in force between nerve and muscle stimulation was 498 used to compute an index of neuromuscular transmission failure (see Methods). The

force loss following repetitive stimulation of muscle directly (Fig. 10D) or the phrenic
nerve (Fig. 10E) was the same in control and DNE preparations. Similarly, the
percentage of the force decline attributable to neuromuscular transmission failure was
the same in both treatment groups (Fig. 10F). Thus, DNE does not impair the
physiology of the neuromuscular junction in diaphragm muscle.

504

505 Discussion

506 Inadvertent obstruction of the airway (e.g., an infant's head covered by bedding) 507 is accompanied by an increase in blood CO_2 and a decrease in O_2 , leading to an 508 increase in the release of several neurotransmitters, including ACh (Metz, 1966). The 509 increased release of excitatory neurotransmitters helps support the respiratory motor 510 response to chemoreceptor stimulation. Here, we found that nicotine exposed neonatal 511 rats had a delayed and blunted genioglossus muscle motor response to nasal airway 512 occlusion, consistent with an attenuation of excitatory drive to XIIMNs under these 513 conditions. We then used an *in vitro* approach to examine excitatory synaptic input to 514 XIIMNs both under baseline conditions and in response to an acute nicotine challenge, 515 which mimics the stimulation of nAChRs that accompanies the release of endogenous 516 ACh, or an increase in central nicotine levels secondary to tobacco smoking or the use 517 of nicotine delivery devices. The key finding is that in 3-5-day old animals, an acute 518 nicotine challenge evoked a marked increase in excitatory synaptic input to XIIMNs in 519 control animals, while the frequency decreased in the DNE pups. Together with 520 previous work showing that nicotine challenge increased GABAergic inhibitory input to 521 XIIMNs (Neff et al., 2003; Jaiswal et al., 2016; Wollman et al., 2018a), these

522	observations suggest that DNE shifts the excitatory-inhibitory balance in XIIMNs
523	towards inhibition in response to a nicotine challenge. This is a deviation from the
524	normal response of neural systems, wherein neuronal spiking activity is maintained
525	within homeostatic limits by careful adjustments in the balance of excitatory and
526	inhibitory synaptic inputs to a neuron or network of neurons (Turrigiano, 2012; Wenner,
527	2014). Below, we discuss how alterations in nAChR function and/or altered
528	development of XIIMNs may underlie the observation that DNE blunts the genioglossus
529	motor response to nasal occlusion and reduces the likelihood of surviving an occlusion.
530	DNE blunts the genioglossus motor response to airway obstruction. Previous
531	work has mainly utilized in vitro techniques to evaluate how DNE alters
532	neurotransmission and the development of hypoglossal motoneurons, which innervate
533	the tongue muscles. In contrast, we are unaware of any studies on the influence of DNE
534	on the control of tongue muscle activity in-vivo. Here, we show that DNE blunts the
535	magnitude and delays the activation of the GG EMG during imposed nasal occlusions.
536	Although we are unable to establish the mechanisms underlying these observations,
537	there are clues from previous work. First, nasal occlusion prevents lung inflation, and
538	the absence of inflation releases hypoglossal motoneurons from inhibition, leading to
539	increased GG activity, at least in adult rodents (Bailey et al., 2001). Second, the
540	previously described reduction in chemosensitivity with DNE in neonatal rodents (St-
541	John and Leiter, 1999; Fewell et al., 2001; Simakajornboon et al., 2004; Hafstrom et al.,
542	2005; Eugenin et al., 2008; Mahliere et al., 2008; Huang et al., 2010) may explain the
543	reduced GG activity during nasal occlusion, as combined hypoxia and hypercapnia
544	become progressively more severe as the occlusion continues and DNE animals are

545 not as well equipped to initiate chemoreceptor-mediated activation of hypoglossal 546 motoneurons. The mechanism of the blunted ventilatory response to chemoreceptor 547 stimulation in nicotine-exposed animals is unknown but could be due to effects on 548 peripheral and central chemoreceptor signaling, and/or a reduced respiratory motor 549 response to the chemoreceptor afferent input. Third, in vitro studies show that DNE is 550 associated with various disruptions in the growth, intrinsic membrane properties and 551 synaptic inputs to hypoglossal motoneurons (Robinson et al., 2002; Pilarski et al., 2011; 552 Jaiswal et al., 2013; Powell et al., 2016; Vivekanandarajah et al., 2016). It is likely that 553 each of the factors contribute in some way to the blunted GG response to nasal 554 occlusion in nicotine exposed pups.

555 We also showed that the majority of pups that failed to recover from nasal 556 occlusion were nicotine exposed. Animals that were used to obtain the main 557 experimental data sets had to meet certain criteria in order for their responses to be 558 analyzed. Criteria included reestablishing inspiratory flow, tidal volume, breathing 559 frequency and EMG activity to baseline levels following nasal occlusions. One hundred 560 and twenty-five animals met these criteria, while 12 did not. Of great interest is that 9 561 out of the 12 animals that failed to recover were nicotine exposed. These findings 562 suggest that DNE may increase the probability that a neonate experiencing an airway 563 occlusion will fail to reestablish a normal breathing pattern, leading to hypoxia and 564 acidosis. An important caveat that envelopes ventilatory measures in neonatal animals 565 is that the stress of maternal separation may interact with DNE and contribute to the 566 altered GG EMG responses observed. Indeed, impaired volitional motor control in DNE 567 animals is exacerbated by maternal separation (Bassey and Gondre-Lewis, 2019).

Influence of DNE on AMPA receptor-mediated glutamatergic neurotransmission.

569 Surprisingly, recordings done under baseline conditions did not reveal 570 differences in the frequency or amplitude of sEPSCs or mEPSCs between control cells 571 and DNE cells at either age. We also assessed postsynaptic receptor function with bath 572 application of AMPA in synaptically isolated neurons. There were no differences in peak 573 AMPA current in control or DNE cells in either age group, and there were no age-574 dependent changes within a treatment group for any of these variables. We note that 575 this approach stimulates both synaptic and extra-synaptic AMPA receptors which may 576 respond differently to DNE. Nevertheless, when taken together with the data showing 577 no change in mESPC amplitude with DNE, the findings indicate that under baseline 578 conditions, DNE does not alter glutamatergic synaptic input to XIIMNs, or the 579 postsynaptic response to AMPA. 580 An important caveat underlying these observations is that previous work showed 581 that the frequency of AMPA receptor-mediated glutamatergic sEPSCs was lower in 582 XIIMNs from DNE cells compared to control cells (Pilarski et al., 2011). However, the 583 latter experiments were done for a different purpose, with recordings made in the setting

584 of elevated extracellular potassium (9 mM) in thick brainstem slices. Moreover,

because the cells were bursting under these conditions, the excitatory inputs could only

586 be discerned in the interburst interval, they were not isolated pharmacologically (i.e.,

inhibitory transmission was intact) and the response to acute nicotine challenge was not
examined. Accordingly, the present results extend these earlier findings.

589 In many physiologic systems underlying pathology is not obvious under baseline 590 conditions but can be revealed when the system is stimulated. It is well known that

568

591	stimulation of nAChRs on glutamatergic neurons leads to increased release of
592	glutamate (Wonnacott et al., 1990; Wonnacott, 1997; Gentry and Lukas, 2002).
593	Importantly, chronic nicotine exposure is associated with both an upregulation and long-
594	term desnensitization of nAChRs in many neuron types (Wonnacott, 1990; Gentry and
595	Lukas, 2002), including XIIMNs (Pilarski et al., 2012); (Wollman et al., 2016).
596	Accordingly, we also studied glutamatergic synaptic transmission while nAChRs were
597	activated with an acute nicotine challenge. Whereas nicotinic stimulation of
598	glutamatergic synaptic transmission was the same in control and DNE pups studied on
599	P1 and P2, there were significant treatment effects in P3-P5 animals. In P3-P5 control
600	animals, acute nicotine challenge increased the frequency of both sEPSCs and
601	mEPSCs, while the frequency of sEPSCs decreased in the DNE animals. Importantly,
602	the stimulation of mEPSCs by acute nicotine challenge in control preparations indicates
603	that nicotine is likely acting on the presynaptic terminals of glutamatergic neurons that
604	impinge upon the motoneurons. The stimulation of sEPSC frequency could involve
605	other sites of nicotine's action, including the soma or dendrites of glutamatergic neurons
606	or neurons presynaptic to them. Nicotine challenge did not affect the mEPSC frequency
607	of P3-5 DNE preparations. Thus, the stimulatory effect on axon terminals at earlier
608	stages may be blunted and/or the reduction in sEPSC frequency at stages P3-5 reflects
609	sites of action other than the presynaptic terminals. Although the mechanisms
610	responsible for the qualitative change in nicotinic control of glutamatergic synaptic
611	transmission in P3-5 animals is unknown, we hypothesize that this is part of the
612	compensatory response to the increased excitability in XIIMNs from nicotine exposed
613	animals (Pilarski et al., 2011; Jaiswal et al., 2013). The 3-5-day delay may reflect the

614	time needed to establish compensatory mechanisms after birth, which is accompanied
615	by a sudden demand for tongue muscle activation to support suckling, licking and
616	swallowing (Thiels et al., 1990). Strategies that neural systems use to compensate for
617	increased excitability could include reducing dendrite volume, increasing pre and/or
618	postsynaptic inhibitory input, or reducing excitatory input. There is evidence that all
619	three adjustments occur in XIIMNs from DNE animals. First, the dendritic tree in XIIMNs
620	from DNE animals is larger and more complex than that of controls on P1-2, but is
621	smaller and less complex by P3-4 (Powell et al., 2016), indicating changes in the timing
622	of growth and pruning of XIIMNs due to DNE. Similarly, DNE may alter the growth and
623	pruning of specific populations of glutamatergic neurons in this region, which could
624	result in altered responses to acute nicotine challenge as seen here. This is supported
625	by work showing that neuronal development is dependent on the trophic effects of ACh,
626	both in utero and into adolescence, and disruption of nicotinic cholinergic signaling in
627	this developmental window alters brain morphology and function, leading to behavioral
628	abnormalities in both humans and animal models (Slotkin et al., 1987; Navarro et al.,
629	1989; Slotkin, 2004). Additionally, changes in the frequency of inhibitory inputs to
630	XIIMNs are known to occur with DNE (Wollman et al., 2018a, b), and DNE is associated
631	with an increase in the postsynaptic response to muscimol in XIIMNs (Wollman et al.,
632	2018a), consistent with an increase in GABA receptor expression (Jaiswal et al., 2016).
633	Other possibilities include inhibitory effects of nAChR activation, activation of GABAB
634	receptors, which were not blocked, or perhaps nicotine-mediated effects on other
635	neuromodulators that inhibit glutamatergic inputs to XII motoneurons, such as serotonin
636	(Singer et al., 1996).

	637	<u>lı</u>
	638	notewor
	639	sEPSCs
4	640	postsyn
Q	641	For exa
1	642	ms, whi
U S	643	conditio
Ď	644	First, the
L	645	it is pos
a B	646	physiolo
\geq	647	be mucl
77	648	DNE me
a)	649	excitato
)t	650	evoked
	651	glyciner
Ű	652	can only
Ŭ	653	by direc
\triangleleft	654	1996; N
0	655	<u>C</u>
	656	have a l
	657	neurom
7	658	fatiguinę
۵ ا	659	hyperpr

rthy finding from these experiments is that the frequency of glutamatergic s invading XIIMNs is lower than the frequency of spontaneous inhibitory aptic currents that have been observed in these cells in previous experiments. imple, glutamatergic sEPSCs in XIIMNs at baseline had an average IEI of 1500 ile GABAergic inputs to XIIMNs had an average IEI of 400 ms under baseline ons (Wollman et al., 2018a). These differences carry two important implications. he data suggest that XIIMNs are under significant inhibition at rest. And second, sible that only small changes in the frequency of glutamatergic inputs have large ogical effects. This could also indicate that the strength of excitatory inputs may h more relevant during periods of high activity than at rest, and therefore the ediated changes may become more pronounced under conditions where bry drive is increased. Interestingly, the reduction in glutamatergic input that is by nicotine challenge in stages P3-5 cannot be due to enhanced GABAergic or rgic inhibition because these were blocked in the current experiments. While we y speculate, it is possible that nicotine evoked a distinct inhibitory effect, either ct action or by causing the release of inhibitory neuromodulators (Singer et al., /laggi et al., 2004).

655 <u>DNE and the integrity of the neuromuscular junction</u>. Adult mammals are said to 656 have a high "safety factor" at the neuromuscular junction, which refers to the ability of 657 neuromuscular transmission to remain effective even under stressful conditions such 658 fatiguing contractions which can occur with elevations in airway resistance or sustained 659 hyperpnea. It is believed that the safety factor is a presynaptic phenomenon, such that

660	the amount of ACh released per nerve impulse exceeds the quantity needed to activate
661	nAChRs and depolarize muscle. However, neuromuscular transmission includes
662	postsynaptic mechanisms as well, and it is possible that DNE alters the function of
663	nAChRs at the neuromuscular junction. Moreover, there is evidence that the safety
664	factor in neonates is lower than in adults due to a relatively low quantal content (Kelly,
665	1978) and more axonal branch point failure (Fournier et al., 1991). Accordingly, we
666	examined the integrity of the neuromuscular junction in control and DNE neonates by
667	stimulating the phrenic nerve repetitively, with periodic superimposition of direct
668	stimulation of muscle fibers. Comparison of the force evoked by phrenic nerve and/or
669	direct stimulation of the muscle fibers showed that DNE had no influence on
670	neuromuscular transmission.
671	An important caveat is that we used the diaphragm muscle for these
672	experiments, rather than the tongue muscles, which are innervated by XIIMNs. Pilot
673	studies showed that measuring force in excised tongue muscles from such small
674	animals is difficult and we were not confident that the measured force was accurate or
675	reproducible. The phrenic nerve-diaphragm preparation did not present these
676	challenges, which explains why it has been an archetypal model for studying the
677	neuromuscular junction.
678	Functional Significance. The consensus explanation for sudden infant death
679	(SIDS) and Apparent Life-Threatening Events (ALTE) is the triple risk hypothesis

680 (Filiano and Kinney, 1994), which is based on the convergence of 1) a vulnerable

neonate (typically due to risks established in utero); 2) a critical developmental period;

682 3) and an exogenous stressor. Maternal smoking is indeed the number one risk factor

683	for SIDS and apparent life threating events in neonates, but the lack of a suitable animal
684	model to probe the mechanisms underlying this association has been elusive. It is
685	noteworthy that SIDS risk is highest in infants aged 4-5 months, while it has been
686	suggested the first two weeks of life in the rat corresponds to 28-40 weeks of gestation
687	in humans (Dwyer et al., 2009), so although the model mimics the triple risk model of
688	SIDS, the developmental discrepancies between rodents and humans make an exact
689	comparison impossible. Nevertheless, we propose that our animal model replicates, at
690	least in part, the triple risk model. Specifically, DNE results in a decrease in nicotine-
691	mediated glutamatergic drive to XIIMNs (vulnerability) at P3-5, but not P1-2 (critical
692	developmental period), and when we imposed airway occlusion (external stressor), the
693	DNE animals had a markedly blunted genioglossus muscle motor response and were
694	less likely to survive the challenge. In summary, the combination of in vitro and in vivo
695	models used here has proven useful in the quest to understand how, and to what
696	extent, maternal smoking/nicotine exposure impairs the function of hypoglossal
697	motoneurons and protective respiratory reflexes.
600	

699 Bibliography

700	Aldrich TK, Shander A, Chaudhry I, Nagashima H (1986) Fatigue of isolated rat diaphragm:
701	role of impaired neuromuscular transmission. J Appl Physiol (1985) 61:1077-1083.
702	Bailey EF, Janssen PL, Fregosi RF (2005) PO2-dependent changes in intrinsic and extrinsic
703	tongue muscle activities in the rat. Am J Respir Crit Care Med 171:1403-1407.
704	Bailey EF, Jones CL, Reeder JC, Fuller DD, Fregosi RF (2001) Effect of pulmonary stretch
705	receptor feedback and CO(2) on upper airway and respiratory pump muscle activity
706	in the rat. J Physiol 532:525-534.
707	Bassey RB, Gondre-Lewis MC (2019) Combined early life stressors: Prenatal nicotine and
708	maternal deprivation interact to influence affective and drug seeking behavioral
709	phenotypes in rats. Behav Brain Res 359:814-822.
710	Berger AJ (2011) Development of synaptic transmission to respiratory motoneurons.
711	Respir Physiol Neurobiol 179:34-42.
712	Berlin I, Heilbronner C, Georgieu S, Meier C, Spreux-Varoquaux O (2010) Newborns' cord
713	blood plasma cotinine concentrations are similar to that of their delivering smoking
714	mothers. Drug Alcohol Depend 107:250-252.
715	Dwyer JB, McQuown SC, Leslie FM (2009) The dynamic effects of nicotine on the
716	developing brain. Pharmacol Ther 122:125-139.
717	Eugenin J, Otarola M, Bravo E, Coddou C, Cerpa V, Reyes-Parada M, Llona I, von Bernhardi R
718	(2008) Prenatal to early postnatal nicotine exposure impairs central
719	chemoreception and modifies breathing pattern in mouse neonates: a probable link
720	to sudden infant death syndrome. J Neurosci 28:13907-13917.
721	Ferng J, Fregosi RF (2015) Influence of developmental nicotine exposure on the ventilatory
722	and metabolic response to hyperthermia. J Physiol 593:5201-5213.
723	Fewell JE, Smith FG, Ng VK (2001) Prenatal exposure to nicotine impairs protective
724	responses of rat pups to hypoxia in an age-dependent manner. Respir Physiol
725	127:61-73.
726	Filiano JJ, Kinney HC (1994) A perspective on neuropathologic findings in victims of the
727	sudden infant death syndrome: the triple-risk model. Biol Neonate 65:194-197.
728	Fournier M, Alula M, Sieck GC (1991) Neuromuscular transmission failure during postnatal
729	development. Neurosci Lett 125:34-36.
730	Gentry CL, Lukas RJ (2002) Regulation of nicotinic acetylcholine receptor numbers and
731	function by chronic nicotine exposure. Curr Drug Targets CNS Neurol Disord 1:359-
732	385.
733	Hafstrom O, Milerad J, Sandberg KL, Sundell HW (2005) Cardiorespiratory effects of
734	nicotine exposure during development. Respir Physiol Neurobiol 149:325-341.
735	Henze DA, Card JP, Barrionuevo G, Ben-Ari Y (1997) Large amplitude miniature excitatory
736	postsynaptic currents in hippocampal CA3 pyramidal neurons are of mossy fiber
737	origin. J Neurophysiol 77:1075-1086.
738	Huang YH, Brown AR, Cross SJ, Cruz J, Rice A, Jaiswal S, Fregosi RF (2010) Influence of
739	prenatal nicotine exposure on development of the ventilatory response to hypoxia
740	and hypercapnia in neonatal rats. J Appl Physiol (1985) 109:149-158.
741	Huckstepp RT, Llaudet E, Gourine AV (2016) CO2-Induced ATP-Dependent Release of
742	Acetylcholine on the Ventral Surface of the Medulla Oblongata. PLoS One
743	11:e0167861.

	744	Jaisv
	745	,
	746	
	747	Jaisv
	748	
	749	Vah
<u></u>	750 751	Kah
	752	
	753	Kell
<u> </u>	754	Lave
$\boldsymbol{\omega}$	755	
10	756	
	757	Low
	758	Mag
	759	
	760 761	Mah
(0)	762	Man
	763	
\geq	764	Met
	765	
	766	Mor
	767	Mor
U	768 769	Mor
	703	MUI
Q	771	Nav
	772	
U	773	
\mathbf{O}	774	Neff
\mathbf{C}	775	
	776	0
	777 778	Otta
	779	
\mathbf{O}	780	Pila
<u> </u>	781	
	782	
	783	Pila
	784	
7	785 786	Dow
	787	Pow
	788	

swal SJ, Pilarski JQ, Harrison CM, Fregosi RF (2013) Developmental nicotine exposure
alters AMPA neurotransmission in the hypoglossal motor nucleus and pre-Botzinger complex of neonatal rats. J Neurosci 33:2616-2625.
iswal SJ, Wollman LB, Harrison CM, Pilarski JQ, Fregosi RF (2016) Developmental nicotine
exposure enhances inhibitory synaptic transmission in motor neurons and
interneurons critical for normal breathing. Dev Neurobiol 76:337-354.
hn A, Groswasser J, Sottiaux M, Kelmanson I, Rebuffat E, Franco P, Dramaix M,
Wayenberg JL (1994) Prenatal exposure to cigarettes in infants with obstructive
sleep apneas. Pediatrics 93:778-783.
elly SS (1978) The effect of age on neuromuscular transmission. J Physiol 274:51-62.
vezzi AM, Corna M, Mingrone R, Matturri L (2010) Study of the human hypoglossal
nucleus: normal development and morpho-functional alterations in sudden
unexplained late fetal and infant death. Brain Dev 32:275-284.
we AA (1980) The neural regulation of tongue movements. Prog Neurobiol 15:295-344.
aggi L, Sola E, Minneci F, Le Magueresse C, Changeux JP, Cherubini E (2004) Persistent decrease in synaptic efficacy induced by nicotine at Schaffer collateral-CA1 synapses
in the immature rat hippocampus. J Physiol 559:863-874.
ahliere S, Perrin D, Peyronnet J, Boussouar A, Annat G, Viale JP, Pequignot J, Pequignot JM,
Dalmaz Y (2008) Prenatal nicotine alters maturation of breathing and neural
circuits regulating respiratory control. Respir Physiol Neurobiol 162:32-40.
etz B (1966) Hypercapnia and acetylcholine release from the cerebral cortex and
medulla. J Physiol 186:321-332.
ortola JP (1984) Breathing pattern in newborns. J Appl Physiol 56:1533-1540.
ortola JP (2004) Implications of hypoxic hypometabolism during mammalian
ontogenesis. Respir Physiol Neurobiol 141:345-356. ortola JP, Tenney SM (1986) Effects of hyperoxia on ventilatory and metabolic rates of
newborn mice. Respiration physiology 63:267-274.
avarro HA, Seidler FJ, Schwartz RD, Baker FE, Dobbins SS, Slotkin TA (1989) Prenatal
exposure to nicotine impairs nervous system development at a dose which does not
affect viability or growth. Brain Res Bull 23:187-192.
eff RA, Wang J, Baxi S, Evans C, Mendelowitz D (2003) Respiratory sinus arrhythmia:
endogenous activation of nicotinic receptors mediates respiratory modulation of
brainstem cardioinhibitory parasympathetic neurons. Circ Res 93:565-572.
taviani G, Matturri L, Mingrone R, Lavezzi AM (2006) Hypoplasia and neuronal
immaturity of the hypoglossal nucleus in sudden infant death. J Clin Pathol 59:497-
500. larski JQ, Wakefield HE, Fuglevand AJ, Levine RB, Fregosi RF (2011) Developmental
nicotine exposure alters neurotransmission and excitability in hypoglossal
motoneurons. J Neurophysiol 105:423-433.
larski JQ, Wakefield HE, Fuglevand AJ, Levine RB, Fregosi RF (2012) Increased nicotinic
receptor desensitization in hypoglossal motor neurons following chronic
developmental nicotine exposure. J Neurophysiol 107:257-264.
well GL, Gaddy J, Xu F, Fregosi RF, Levine RB (2016) Developmental nicotine exposure
disrupts dendritic arborization patterns of hypoglossal motoneurons in the neonatal
rat. Dev Neurobiol 76:1125-1137.

700	Demman IF de Creat MI Couerland FK Angle AM (1070) Dethagenegis of unner simular
789 790	Remmers JE, deGroot WJ, Sauerland EK, Anch AM (1978) Pathogenesis of upper airway
	occlusion during sleep. J Appl Physiol Respir Environ Exerc Physiol 44:931-938. Rice A, Fuglevand AJ, Laine CM, Fregosi RF (2011) Synchronization of presynaptic input to
791	
792	motor units of tongue, inspiratory intercostal, and diaphragm muscles. J
793	Neurophysiol 105:2330-2336.
794	Robinson DM, Peebles KC, Kwok H, Adams BM, Clarke LL, Woollard GA, Funk GD (2002)
795	Prenatal nicotine exposure increases apnoea and reduces nicotinic potentiation of
796	hypoglossal inspiratory output in mice. J Physiol 538:957-973.
797	Sant'Anna GM, Mortola JP (2003) Thermal and respiratory control in young rats exposed to
798	cold during postnatal development. Comparative biochemistry and physiology Part
799	A, Molecular & integrative physiology 134:449-459.
800	Semple BD, Blomgren K, Gimlin K, Ferriero DM, Noble-Haeusslein LJ (2013) Brain
801	development in rodents and humans: Identifying benchmarks of maturation and
802	vulnerability to injury across species. Prog Neurobiol 106-107:1-16.
803	Simakajornboon N, Vlasic V, Li H, Sawnani H (2004) Effect of prenatal nicotine exposure on
804	biphasic hypoxic ventilatory response and protein kinase C expression in caudal
805	brain stem of developing rats. J Appl Physiol (1985) 96:2213-2219.
806	Singer JH, Bellingham MC, Berger AJ (1996) Presynaptic inhibition of glutamatergic
807	synaptic transmission to rat motoneurons by serotonin. J Neurophysiol 76:799-807.
808	Slotkin TA (2004) Cholinergic systems in brain development and disruption by
809	neurotoxicants: nicotine, environmental tobacco smoke, organophosphates. Toxicol
810	Appl Pharmacol 198:132-151.
811	Slotkin TA, Orband-Miller L, Queen KL (1987) Development of [3H]nicotine binding sites in
812	brain regions of rats exposed to nicotine prenatally via maternal injections or
813	infusions. J Pharmacol Exp Ther 242:232-237.
814	St-John WM, Leiter JC (1999) Maternal nicotine depresses eupneic ventilation of neonatal
815	rats. Neurosci Lett 267:206-208.
816	Thiels E, Alberts JR, Cramer CP (1990) Weaning in rats: II. Pup behavior patterns. Dev
817	Psychobiol 23:495-510.
818	Turrigiano G (2012) Homeostatic synaptic plasticity: local and global mechanisms for
819	stabilizing neuronal function. Cold Spring Harb Perspect Biol 4:a005736.
820	Vivekanandarajah A, Chan YL, Chen H, Machaalani R (2016) Prenatal cigarette smoke
821	exposure effects on apoptotic and nicotinic acetylcholine receptor expression in the
822	infant mouse brainstem. Neurotoxicology 53:53-63.
823	Wenner P (2014) Homeostatic synaptic plasticity in developing spinal networks driven by
824	excitatory GABAergic currents. Neuropharmacology 78:55-62.
825	Wollman LB, Levine RB, Fregosi RF (2018a) Developmental plasticity of GABAergic
826	neurotransmission to brainstem motoneurons. J Physiol 596:5993-6008.
827	Wollman LB, Levine RB, Fregosi RF (2018b) Developmental nicotine exposure alters
828	glycinergic neurotransmission to hypoglossal motoneurons in neonatal rats. J
829	Neurophysiol 120:1135-1142.
830	Wollman LB, Haggerty J, Pilarski JQ, Levine RB, Fregosi RF (2016) Developmental nicotine
831 832	exposure alters cholinergic control of respiratory frequency in neonatal rats. Dev
832	Neurobiol 76:1138-1149.
833	Wonnacott S (1990) The paradox of nicotinic acetylcholine receptor upregulation by
834	nicotine. Trends Pharmacol Sci 11:216-219.

	835 836 837 838 839	 Wonnacott S (1997) Presynaptic nicotinic ACh receptors. Trends Neurosci 20:92-98. Wonnacott S, Sidhpura N, Balfour DJ (2005) Nicotine: from molecular mechanisms to behaviour. Curr Opin Pharmacol 5:53-59. Wonnacott S, Drasdo A, Sanderson E, Rowell P (1990) Presynaptic nicotinic receptors and the modulation of transmitter release. Ciba Found Symp 152:87-101; discussion 102, 105.
	840 841	102-105. Wood SJ, Slater CR (2001) Safety factor at the neuromuscular junction. Prog Neurobiol
0	842 843	64:393-429. Zhan WZ, Watchko JF, Prakash YS, Sieck GC (1998) Isotonic contractile and fatigue
-	844	properties of developing rat diaphragm muscle. J Appl Physiol (1985) 84:1260-
	845 846	1268. Figure and Table legends
5	847	Table 1. List of drug cocktails used to isolate AMPA receptor-mediated
	848	glutamatergic EPSCs and postsynaptic AMPA receptors, with the number of cells used
	849	in each condition. The number of cells studied in each experiment are also shown.
5	850	Table 2. Statistical tests and significance threshold used for each experiment in
	851	each experimental series.
J	852	Table 3. Age, weight, resting membrane potential (mV), and input resistance
L L	853	(Rin) of XIIMNs from control and DNE animals. Values are mean \pm SD. There were no
0	854	differences in any of these variables between control and DNE cells. The only
U U	855	significant differences between P1-P2 and P3-P5 within a treatment group was body
	856	weight, as expected. ***, P<0.001, P1-P2 vs. P3-P5 within a treatment group.
1	857	Table 4. Number of sEPSCs and mEPSCs recorded per neuron at baseline and
	858	during acute nicotine application. Values are mean ± SD.
	859	Table 5. Mean values for amplitude of glutamatergic sEPSCs, mEPSCs and
\supset	860	mEPSC rise time at baseline and during acute nicotine challenge. There were no
eNeC	861	significant differences in any of these variables.
	862	

aNauro Arcantad Manuscrint

863	Figure 1. In vivo experimental model and EMG response to nasal occlusion.
864	Panel A. Schematic rendition of the in vivo experimental preparation, which combines
865	head-out plethysmography and genioglossus EMG recordings in lightly anesthetized
866	neonatal rats, as described in Methods. Panel B. Example trace showing diaphragm
867	and genioglossus EMG and integrated EMG along with volume and flow traces obtained
868	from the plethysmograph. After 5 minutes of uninterrupted baseline recordings, a 10-15
869	second nasal occlusion was administered (rectangle). Panel C. Genioglossus (GG)
870	EMG amplitude during the nasal occlusion. The duration of the nasal occlusion was
871	normalized by dividing the total duration of each occlusion into equal 20%-time bins.
872	EMG amplitude was normalized as a percent of the largest burst recorded (see
873	Methods). All animals in both groups showed increased GG burst amplitude as the
874	nasal occlusion progressed. Post hoc analysis following 2-way ANOVA revealed that
875	DNE animals had a significantly blunted amplitude response compared to control at the
876	40%, 60%- and 80%-time bins. *, P< 0.05, **P< 0.01, ***, P< 0.001.
877	Figure 2. Elapsed time between the onset of nasal occlusion to first
878	discernible genioglossus muscle EMG burst, defined as onset latency. Panel A
879	shows recordings from representative control and DNE pups, as indicated. The length
880	of the blue line under the EMG tracing represents the latency, which is prolonged in the
881	DNE animal. following the onset of nasal occlusion. Panel B shows the onset latency in
882	9 control and DNE pups. The horizontal lines represent the mean value. An unpaired t-
883	test revealed a significant difference between the groups (***, P< 0.001).
884	Figure 3. Failure to recover from nasal occlusion. Panel A. An example
885	tracing of one of the 12 animals that exhibited continuous breathing difficulties post

nasal occlusion, as explained in Results. *Panel B*. The number of animals in each
treatment group that either recovered from nasal occlusion or failed to recover. Note
that of the 12 animals that failed to recover, 9 were from the DNE group, which is a
significant difference by Chi square analysis (P = 0.0290).

890 Figure 4. Example traces of AMPA receptor-mediated sEPSCs recorded 891 from XIIMNs. Panels A and B show representative traces of pharmacologically isolated 892 sEPSCs from a control animal (Panel A) and a DNE animal (Panel B), both studied on 893 P4. Each trace shows the entire three-minute recording period at baseline (upper trace 894 in each panel) and during acute nicotine application (bottom trace in each panel). Inset 895 panels are an expanded view, showing 10 seconds of the recording at the end of each 896 trace. Note that the size and frequency of events at baseline is similar in the control and 897 DNE animals. In contrast, with acute nicotine challenge (bottom trace in each panel) the 898 DNE cell shows a decrease in sEPSC frequency, whereas there is a modest increase in 899 the control cell.

Figure 5. DNE alters the modulation of glutamatergic sEPSCs in response
to an acute nicotine challenge, but only in cells from pups aged P3-P5.

Cumulative probability distributions of glutamatergic sEPSC IEIs in control and DNE
cells, at baseline and during acute nicotine challenge. At P1-2 (Panels A and B), acute
nicotine challenge with 0.5 μM nicotine (black dashed lines) caused a left shift, toward
shorter IEIs, of glutamatergic sEPSCs in both control and DNE cells (Control, P=0.049,
Panel A; DNE, P<0.0001, Panel B). In cells from P3-P5 animals (Panels C and D),
acute nicotine challenge caused a left shift, toward shorter IEIs in control cells
(P<0.0001, Panel C), the distribution shifted to the right, towards longer IEIs in the DNE

909

910 challenge and indicates significant differences with K-S test (See Methods). Dotted 911 gray lines indicate the 95% confidence intervals of each curve. 912 Figure 6. Influence of DNE on AMPA receptor-mediated mEPSCs recorded 913 from XIIMNs. Panels A and B show representative traces of pharmacologically isolated 914 mEPSCs from a control animal (Panel A) and a DNE animal (Panel B) studied on P4. 915 Each trace shows the entire three minutes of recording at baseline (top trace) and 916 during acute nicotine application (bottom trace). Inset panels show an expanded view of 917 10 seconds at the end of each trace, as in Fig. 4 Note that the size and frequency of 918 events is similar in the control and DNE cell at baseline. However, during acute nicotine 919 challenge, mEPSC frequency increased in control cells but not in DNE cells. 920 Figure 7. Cumulative probability distributions of glutamatergic mEPSC IEIs 921 in control and DNE cells, at baseline and during acute nicotine challenge. In cells 922 from animals aged P1-2 (Panels A and B), acute nicotine challenge with 0.5 μM 923 nicotine (black dashed lines) caused a left shift, toward shorter IEIs, of glutamatergic 924 mEPSCs in both control (P<0.0001, Panel A) and DNE cells (P<0.0001, Panel B). In 925 cells from animals aged P3-5 (Panels C and D), acute nicotine challenge caused a 926 significant left shift of glutamatergic mEPSCs in control cells (P=0.004, Panel C), but 927 there was no change in the distribution of IEIs in DNE cells (P=0.066, Panel D). Arrows 928 indicate the direction of the shift with acute nicotine challenge and indicates significant 929 differences with K-S test (See Methods). Dotted gray lines indicate the 95% confidence 930 intervals of each curve.

cells (P=0.012, Panel D). Arrows indicate the direction of the shift with acute nicotine

931	Figure 8. Individual and average IEI of sEPSCs and mEPSCs at baseline
932	and during acute nicotine challenge. Panel A shows the individual and average IEI of
933	AMPA receptor-mediated sEPSCs under baseline conditions and following acute
934	nicotine challenge. Note that in control cells (circles, left of the vertical line) there was a
935	slight though non-significant decline in IEI (i.e., an increase in frequency) on both P1-P2
936	(filled circles) and P3-P5 (open circles). The IEI in response to an acute nicotine
937	challenge in cells from DNE animals was age-dependent (squares, right of the vertical
938	line). Note that on P1-P2, nicotine challenge decreased the IEI, though as in controls
939	this trend was not significant. Surprisingly, on P3-P4 acute nicotine challenge
940	significantly increased the IEI (P = 0.0021). Moreover, the mean value for IEI in P3-5
941	DNE cells during acute nicotine challenge is significantly different than corresponding
942	data in P1-2 DNE cells (P = 0.0001), and in P3-5 cells from control animals. Panel B
943	shows the individual and average IEI of AMPA receptor-mediated mEPSCs under
944	baseline conditions and following acute nicotine challenge. Note that in the P1-2 group,
945	both control and DNE cells show a trend toward a decrease in IEI with acute nicotine
946	challenge, however this was not significant. Analysis of average IEI from control and
947	DNE neurons at P3-5 shows no differences at baseline and no change in frequency with
948	acute nicotine challenge.
949	Figure 9. Activation of postsynaptic AMPA receptors in control cells and

DNE cells. Panel A shows a representative trace of the AMPA receptor mediated inward current in XIIMNs from a control animal at P1. **Panel B** shows individual values for the peak inward current in response to bath application of AMPA. Mean values within each treatment group are indicated by the horizontal lines. There were no

954 differences in the magnitude of the postsynaptic inward current either within or between955 treatment groups.

956 Figure 10. Influence of DNE on diaphragm muscle fatigue and 957 neuromuscular transmission failure during repetitive muscle or phrenic nerve 958 stimulation in diaphragm phrenic nerve-muscle strips. Panel A shows 959 representative force recording over a 5-minute period of direct muscle stimulation. 960 Fatigue was quantified as the % of the maximum force remaining at the end of the 5-961 minute stimulation period (see Methods). Panel B shows the muscle twitch produced 962 by a single stimulus pulse, and an expanded view of the muscle force produced by a 963 330 ms train of stimulation pulses, as described in Methods. An identical protocol was 964 used when phrenic nerve stimulation was used to assess the magnitude of force 965 decline. Panel C shows representative force recording during 5 minutes of repeated 966 phrenic nerve stimulation with superimposed direct muscle stimulation every 15 sec. 967 Neuromuscular transmission failure (NTF) was calculated as: Panels D and E show the 968 percent force decline in each control and DNE preparation subjected to either muscle 969 (Panel D) or phrenic nerve (Panel E) stimulation. Panel F shows the percent 970 neuromuscular transmission failure in control and DNE preparations. Horizontal lines in 971 Panels D, E and F indicate the mean. There were no significant differences in the 972 percent force loss between control and DNE preparations with either muscle or nerve 973 stimulation, or the force loss due to neuromuscular transmission failure. 974

975

976 977

TABLE 1. List of drug cocktails used to isolate AMPA receptor-mediated

980 glutamatergic EPSCs and postsynaptic AMPA receptors, with the number of cells used

981 in each condition. The number of cells studied in each experiment are also shown.

Experiments and drugs used	Age	# Cells (Control:DNE)
Glutamate sEPSCs 50 μM AP-5, 10 μM bicuculline, 0.4 μM strychnine + 0.5 μM nicotine	P1-2 P3-5	6:6 6:6
Glutamate mEPSCs 50 μM AP-5, 10 μM bicuculline, 0.4 μM strychnine, 1 μM tetrodotoxin (TTX) + 0.5 μM nicotine	P1-2 P3-5	6:6 6:6
Postsynaptic receptors 50 μM AP-5, 10 μM bicuculline, 0.4 μM strychnine, 1 μM TTX + 2.5 μM AMPA	P1-2 P3-5	6:6 6:6

TABLE 2. Statistical tests and significance threshold used for each experiment

1005 in each experimental series.

Experiment	Statistical test, post hoc	Significance Threshold
In vivo series 1. Changes to EMG during nasal occlusion	Two-way mixed-model ANOVA with Tukey's post-hoc analysis	P < 0.05
2. Differences in EMG onset latency	Unpaired Student's t-test	P < 0.05

3.	Autoresuscitation	Chi Squared analysis	P < 0.05
_	o series A Differences in baseline parameters	Two-way mixed model ANOVA with Tukey's post-hoc analysis	P < 0.05
2.	Differences in IEI and amplitude of EPSCs	Kolomogorov-Smirnoff test of cumulative probability distributions, and Three-way mixed model ANOVA with the Holm-Sidak post- hoc analysis	P < 0.05
3.	Differences in peak whole cell current	Unpaired Student's t-test	P < 0.05
In vitr	o series B		
1.	Differences in nerve stimulation, muscle stimulation, and estimates of neuromuscular transmission failure	Unpaired Student's t-test	P < 0.05

eNeuro Accepted Manuscript

1023
1024
1025 **TABLE 3.** Age, weight, resting membrane potential (mV), and input resistance (Rin) of XIIMNs from control and DNE animals.

	Control	DNE	P Value	n
				(Control:DNE)
Age (days)				
P1-2	1.7±0.2	1.4±0.1	P= n/s	18:18
P3-5	3.4±0.1	3.7±0.2	P= n/s	18:18
Weight (grams)				
P1-2	7.72±0.31	7.4±0.1	P= n/s	18:18
P3-5	10.53±0.44***	10.8±0.3***	P= n/s	18:18
Vm				
P1-2	-49±3	-48±2	P= n/s	18:18
P3-5	-48±2	-47±2	P= n/s	18:18
Rin (MΩ)				
P1-2	221±49	184±23	P= n/s	4:4
P3-5	185±41	189±42	P= n/s	4:4

eNeuro Accepted Manuscript

1047
1048
1049
1050
1051
1052
1053
1054
1055 **Table 4.** Number of sEPSCs and mEPSCs recorded per neuron at baseline and during acute nicotine application. Values are mean ± SD.
1057

SEPSCs

SLFUUS	
P1-2	

Baseline	65±23	91±38
Acute nicotine	74±59	187±105
P3-4		
Baseline	145±107	116±84
Acute nicotine	211±211	81±60

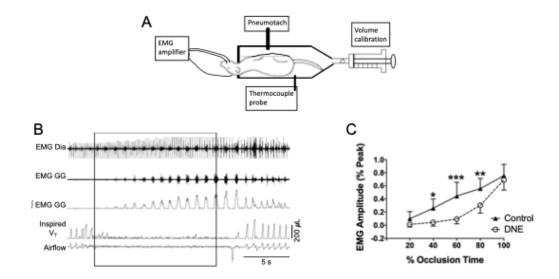
1061 1062

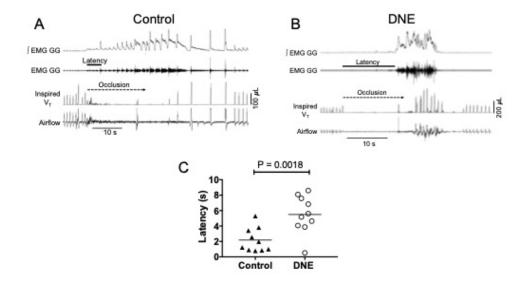
mESPCs		
P1-2		
Baseline	28±14	28±22
Acute nicotine	38±20.8	61±39
P3-4		
Baseline	18±13	41±38
Acute nicotine	31±15	33±27

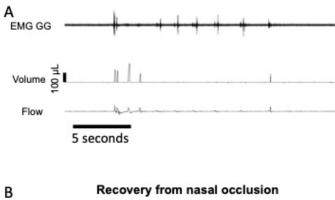
TABLE 5. Mean values for amplitude of glutamatergic sEPSCs, mEPSCs and
 mEPSC rise time at baseline and during acute nicotine challenge. There were no
 significant differences in any of these variables.

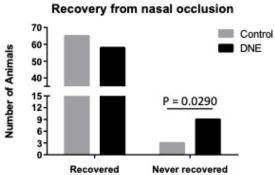
	Baseline	Acute nicotine challenge
sEPSC Amplitude (pA)		
Control:		
P1-2	-15.2 ± 2.7	-16.0 ± 3.2
P3-5	-15.5 ± 2.3	-15.7 ± 3.9
DNE:		
P1-2	-18.5 ± 7.4	-18.3 ± 8.9
P3-5	-16.4 ± 2.8	-14.8 ± 2.9
mEPSC Amplitude (pA)		
Control:		
P1-2	-16.2 ± 2.6	-14.6 ± 2.6
P3-5	-14.9 ± 3.0	-16.3 ± 3.7
DNE:		
P1-2	-16.0 ± 2.9	
P3-5	-17.5 ± 1.9	-17.4 ± 1.9
mEPSC rise time (msec)		
<u>Control</u> :		
P1-2	2.1 ± 0.2	2.1 ± 0.2
P3-5	2.0 ± 0.1	2.2 ± 0.1
DNE:		
P1-2	2.1 ± 0.2	2.0 ± 0.1
P3-5	1.8 ± 0.1	2.0 ± 0.1



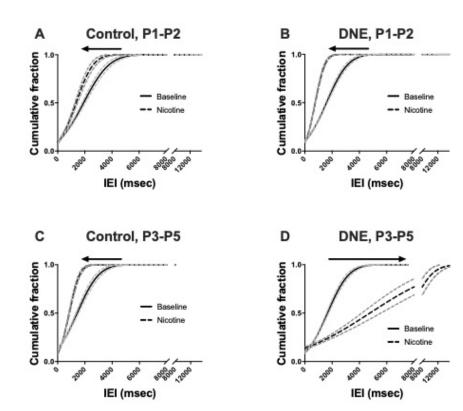


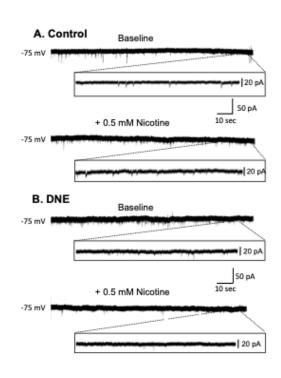


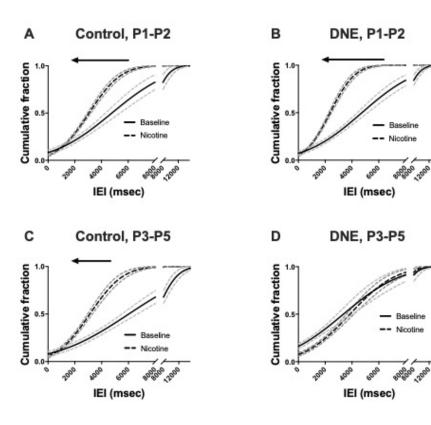




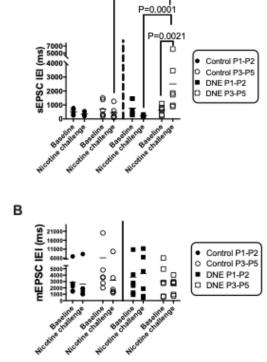
A. Control	Baseline
-75 mV	an and a second second second second second
***	150 pA
	+ 0.5 mM Nicotine 10 sec
-75 mV	and the second
	50 pA
B. DNE	Baseline
-75 mV	and the second s
	50 pA
	+ 0.5 mM Nicotine 10 sec
-75 mV	
	50 pA







eNeuro Accepted Manuscript



P=0.0006

Α

